Letter

Quantum spin state stabilized by coupling with classical spins

H. Yamaguchi,[1,*] T. Okubo,[2] A. Matsuo,[3] T. Kawakami,[4] Y. Iwasaki,[5] T. Takahashi,[1] Y. Hosokoshi,[1] and K. Kindo[3]

[1]*Department of Physics, Osaka Metropolitan University, Osaka 599-8531, Japan*
[2]*Department of Physics, the University of Tokyo, Tokyo 113-0033, Japan*
[3]*Institute for Solid State Physics, the University of Tokyo, Chiba 277-8581, Japan*
[4]*Department of Chemistry, Osaka University, Toyonaka, Osaka 560-0043, Japan*
[5]*Department of Physics, College of Humanities and Sciences, Nihon University, Tokyo 156-8550, Japan*

(Received 4 August 2023; accepted 29 February 2024; published 15 March 2024)

We introduce a model compound featuring a spin-1/2 frustrated square lattice partially coupled by spin-5/2. A significant magnetization plateau exceeding 60 T could be observed, indicating a quantum state formed by $S = 1/2$ spins in the square lattice. The remaining $S = 5/2$ spins exhibited paramagnetic behavior in the low-field regions. The numerical analysis confirmed that the observed quantum state is a many-body entangled state based on the dominant antiferromagnetic interactions and is strongly stabilized by coupling with spin-5/2. The stabilization of this quantum state can be attributed to a compensation effect similar to magnetic field-induced superconductivity, which serves as a strategy to control the stability of quantum spin states in magnetic fields.

DOI: 10.1103/PhysRevB.109.L100404

Quantum spins in condensed-matter physics give rise to various entangled states, thus facilitating the studies on quantum computation achieved through single-qubit measurements on quantum spin states [1,2]. The main objective is to stabilize various quantum states in spin systems to serve as resources. The gain of the magnetic energy through the formation of quantum states could be essential to quantize magnetic states in condensed-matter systems. As a representative example, frustrated spin systems with competing exchange interactions induce quantum states to lower the ground-state energy by suppressing the development of the magnetic moment. Extraordinary quantum states, such as the quantum spin liquid and the spin nematic, are proposed in low-dimensional frustrated systems [3–5]. If there is no frustration, slight perturbations, such as lattice distortion [6–8] and bond randomness [9], in 2D systems can easily stabilize quantum states. Even in one-dimensional (1D) systems with strong quantum fluctuations, highly entangled nonmagnetic quantum states are preferentially formed. The singlet state in the antiferromagnetic (AF) spin-1/2 chain with the lattice alternation, which corresponds to the dominant correlation in the present study, has lower energy than the ground state in the uniform AF chain. In some 1D chain compounds, such singlet states can be formed even by distorting the lattice at a certain temperature, leading to a spin-Peierls transition [10–14].

The flexibility of molecular orbitals in organic radical systems can generate advanced spin-lattice designs, leading to realization of a variety of quantum spin states. Our previous attempts in spin-lattice design using verdazyl-based quantum organic materials (V-QOM) have resulted in the formation of diverse quantum spin systems, including ferromagnetic-leg ladders [15–17], quantum pentagon [18], honeycomb with randomness [19], and frustrated square lattices [20–23], which were not achievabe with conventional organic and inorganic materials. These spin models formed through V-QOM lead to unconventional quantum states that originate from highly entangled spins. The next stage in spin-lattice design using V-QOM involves the synthesis of verdazyl-based salts by combining cationized verdazyl radicals with magnetic anions. This approach is aimed at achieving more diverse quantum spin states through the coupling between π electrons in the radicals and $3d$ electrons in the anion molecules (π-d interaction). This coupling results in magnetic field-induced quantum behavior [24,25] and the Lieb-Mattice ferrimagentic state [26–28]. In the realm of π-d systems, organic conductors with conducting π electrons and localized d spins were extensively investigated, particularly magnetic field-induced superconductivity [29,30], wherein the polarized d spins stabilized the superconductivity by inducing an effective zero-field condition in the π site [31]. Similarly, in the present work, the quantum state formed in the radical salt is also expected to be stabilized through a similar mechanism through π-d interactions.

In this Letter, we present a model compound featuring a spin-1/2 spatially anisotropic frustrated square lattice partially coupled with spin-5/2. Single crystals of the verdazyl-based salt (m-MePy-V)$_2$MnCl$_4$ were successfully synthesized. Molecular orbital (MO) calculations revealed four types of exchange interactions, forming the spin-1/2 square lattice and partially coupling with spin-5/2. High-field measurements indicate a significant magnetic plateau exceeding 60 T, indicating the formation of a nonmagnetic quantum state by $S = 1/2$ spins in the square lattice. Numerical analysis demonstrates that this observed quantum state exhibits singletlike correlation and is strongly stabilized by the coupling with spin-5/2.

To prepare m-MePy-V, we used a conventional procedure [32] and (m-MePy-V)$_2$MnCl$_4$ was synthesized

*Corresponding author: h_yamaguchi@omu.ac.jp

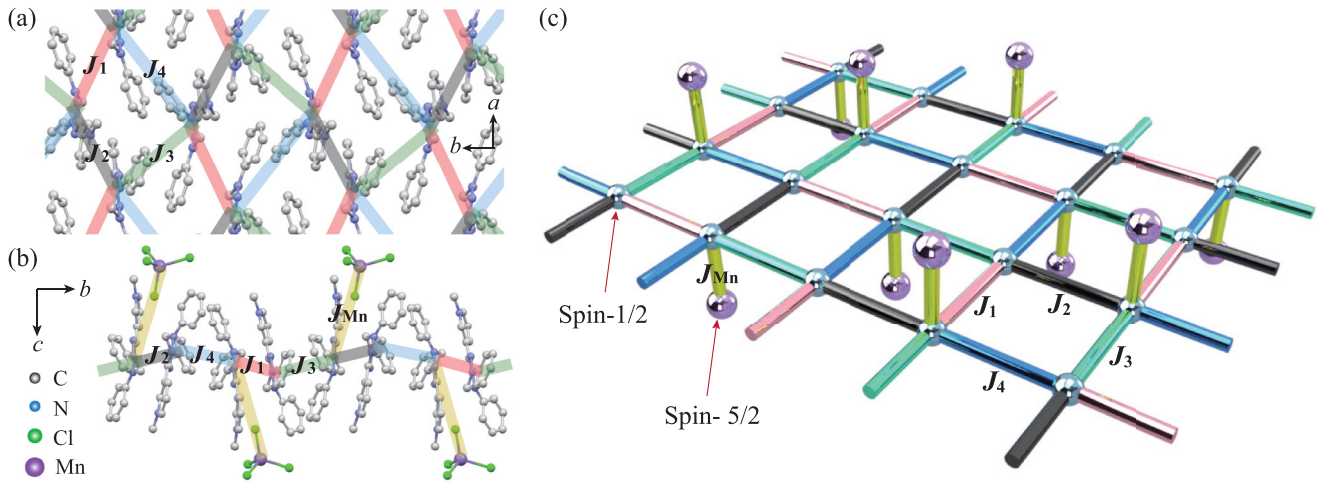

FIG. 1. (a) Crystal structure of $(m\text{-MePy-V})_2MnCl_4$ in the (a) *ab* and (b) *bc* planes. Hydrogen atoms are omitted for clarity. The broken lines represent the bonds forming the spin lattice. (c) Two-dimensional spin model in the *ab* plane. J_1, J_2, J_3, and J_4 form the frustrated square lattice of $S = 1/2$ spins and one of two $S = 1/2$ sites is coupled by $S = 5/2$ spins through J_{Mn}.

following a reported method for salts with similar chemical structures [22,33]. The dark-brown $(m\text{-MePy-V})_2MnCl_4$ crystals were obtained through recrystallization using methanol. The crystal structure was determined from intensity data collected using a Rigaku AFC-8R Mercury CCD RA-Micro7 diffractometer. High-field magnetization measurements were carried out using a nondestructive pulse magnet, subjecting the samples to pulsed magnetic fields of up to approximately 60 T. The magnetic susceptibility was measured using a commercial SQUID magnetometer (MPMS-XL, Quantum Design). The experimental results were corrected considering the diamagnetic contributions calculated via Pascal's method. Specific heat measurements were performed using a commercial calorimeter (PPMS, Quantum Design). All experiments were conducted on small randomly oriented single crystals, considering the isotropic nature of organic radical systems.

The verdazyl radical *m*-MePy-V and $MnCl_4$ anion have spin-1/2 and 5/2, respectively [34]. The crystallographic parameters at room temperature are as follows: monoclinic, space group $P2_12_12_1$, $a = 10.6892(3)$ Å, $b = 15.2412(4)$ Å, $c = 24.4578(7)$ Å, $V = 3984.57(19)$ Å^3, $Z = 4$, $R = 0.0389$, and $R_w = 0.1003$. We performed MO calculations [35] to evaluate the exchange interactions. Subsequently, four types of dominant interactions were found between the $S = 1/2$ spins on the radicals [34], as shown in Fig. 1(a). They are identified as $J_1/k_B = 72$ K, $J_2/k_B = 45$ K, $J_3/k_B = 12$ K, and $J_4/k_B = -8$ K, which are defined in the Heisenberg spin Hamiltonian given by $\mathcal{H} = J_n \sum_{\langle i,j \rangle} S_i \cdot S_j$, where $\sum_{\langle i,j \rangle}$ denotes the sum over the neighboring spin pairs. Moreover, one dominant AF interaction, J_{Mn}, is expected between spin-1/2 and -5/2 [34], as shown in Fig. 1(b). Considering that the evaluation of absolute values of interactions between radical and $MnCl_4$ anion is difficult, we roughly evaluated as $J_{Mn}/J_1 \simeq 0.2$ using the following analysis of magnetic susceptibility. Consequently, $S = 1/2$ spins form a spatially anisotropic square lattice through J_1–J_4 in the *ab* plane, to which $S = 5/2$ spins are partially connected, as shown in Fig. 1(c). Each square unit has frustration caused by three AF interactions and one ferromagnetic interaction, which is divided into the following two patterns: J_1-J_2-J_3-J_4 and J_1-J_3-J_4-J_2.

Figure 2(a) shows the temperature dependence of the magnetic susceptibility ($\chi = M/H$) at 0.1 T, revealing a monotonic paramagnetic increase with decreasing temperatures. In the high-temperature region, χT exhibits a rounded minimum at approximately 20 K, as shown in the inset of Fig. 2(a). This behavior is typical of mixed spin systems [26,37–39], where interactions between spins of different sizes lead to excited states composed of smaller effective spins than those in the ground state, resulting in a rounded minimum in χT. In our system, the χT behavior strongly depends on the value of J_{Mn} between spin-1/2 and -5/2. Based on MO calculations that indicate J_1 to be the most dominant interaction between $S = 1/2$ spins, we assumed a spin-(1/2,1/2,5/2) trimer coupled by J_1 and J_{Mn} with the spin Hamiltonian given by $\mathcal{H} = J_1 S_{V1} \cdot S_{V2} + J_{Mn} S_{V2} \cdot S_{Mn}$, where S_{Vi} and S_{Mn} are the spin-1/2 and spin-5/2 operators, respectively. The calculated results, as shown in the inset of Fig. 2(a), well reproduce the rounded minimum, allowing us to evaluate $J_{Mn}/J_1 \simeq 0.2$.

Figure 2(b) displays the magnetization curve at 4.2 K measured in pulsed magnetic fields, with its inset showing the low-field region measured in static magnetic fields. The observed hysteresis in pulsed magnetic fields originates from the slow relaxation characteristic of organic radical systems. The magnetization gradually increases up to a value of $5\mu_B$/f.u., which persists up to at least 60 T. Considering the isotropic g values (∼2.0) of the verdazyl radical and Mn^{2+} ion, the saturation value is expected to be $7\mu_B$/f.u. Therefore, the magnetic moment of $5\mu_B$/f.u. corresponds to the full polarization of spin-5/2 along the field direction, representing 5/7 of the full saturation value. The gradual increases in the low-field region can be effectively explained by the Brillouin function for the spin-5/2 monomer, as shown in Fig. 2(b). These behaviors suggest that the $S = 1/2$ spins in the square lattice form a nonmagnetic quantum state.

The temperature dependence of the specific heat C_p is shown in Fig. 3(a). No peak indicative of a phase transition to a magnetic order is observed, but a significant change occurs

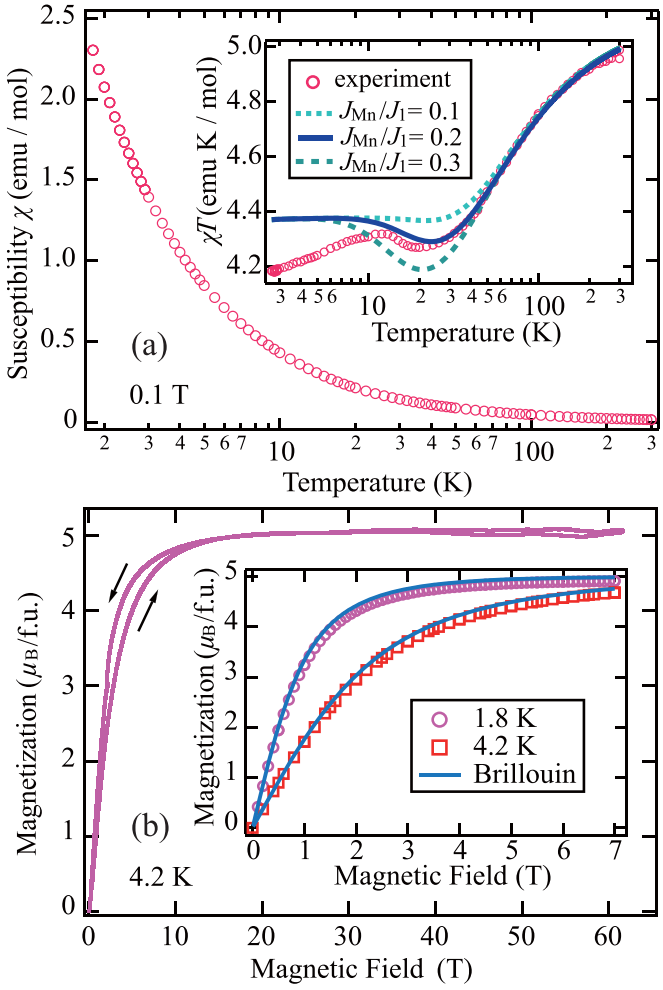

FIG. 2. (a) Temperature dependence of the magnetic susceptibility ($\chi = M/H$) of (m-MePy-V)$_2$MnCl$_4$ at 0.1 T. The inset shows the temperature dependence of χT. The lines represent the calculated results for the spin-(1/2,1/2,5/2) trimer coupled by J_1 and $J_{\rm Mn}$. (b) Magnetization curves of (m-MePy-V)$_2$MnCl$_4$ at 4.2 K in pulsed magnetic fields. The inset shows the low-field region measured in static magnetic fields at 1.8 and 4.2 K. The solid lines represent the Brillouin function for spin-5/2.

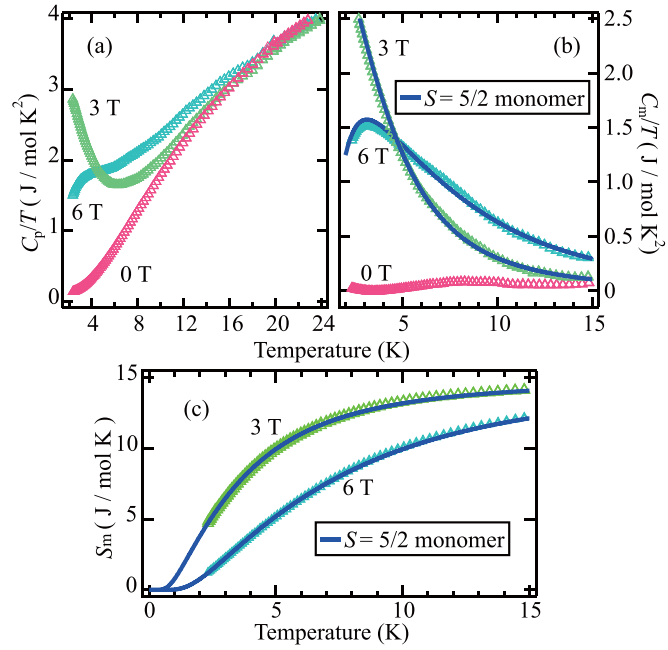

FIG. 3. (a) Temperature dependence of the specific heat $C_{\rm p}/T$ of (m-MePy-V)$_2$MnCl$_4$ at 0, 3, and 6 T. (b) Low-temperature region of $C_{\rm m}/T$. The solid lines represent the Schottky-type specific heat originating from the Zeeman splitting of spin-5/2. (c) Temperature dependence of the magnetic entropy $S_{\rm m}$. The experimental values for 3 and 6 T have been shifted up by 4.7 and 1.2 J/mol K, respectively, to overlap with the calculated results.

below approximately 15 K when magnetic fields are applied. As the low-temperature magnetization exhibits spin-5/2 paramagnetic behavior, the strong magnetic field dependence of $C_{\rm p}$ is considered to originate from the Zeeman splitting of spin-5/2, leading to Schottky contributions when magnetic fields are applied. To evaluate the Schottky-type specific heat, we assumed Zeeman energy given by $-g\mu_B S_z$, where $S_z = \pm 5/2, \pm 3/2, \pm 1/2$. Furthermore, the magnetic specific heat $C_{\rm m}$ was determined by subtracting the lattice contribution $C_{\rm l}$ from the experimental results. Below 15 K, $C_{\rm l}$ was approximated as $C_{\rm l} = a_1 T^3 + a_2 T^5 + a_3 T^7$, a form that has been confirmed to be effective for verdazyl-based compounds [40,41]. The constants $a_1 - a_3$ were determined to reproduce the calculated Schottky-type specific heat. As shown in Fig. 3(b), the magnetic specific heats at 3 T and 6 T are well explained by the calculated results assuming $C_{\rm l}$ with $a_1 = 0.022$, $a_2 = -5.6 \times 10^{-5}$, and $a_3 = 5.1 \times 10^{-8}$. The value of a_1 corresponds to a Debye temperature of 44 K, consistent with those used for other verdazyl-based compounds [15,16,22,40]. The evaluated $C_{\rm m}$ at zero field is quite small, further supporting that the observed specific heats mainly originate from the Zeeman splitting of spin-5/2. Figure 3(c) shows the magnetic entropy $S_{\rm m}$ obtained via the integration of $C_{\rm m}/T$, where the experimental data for 3 and 6 T have been shifted up by 4.7 and 1.2 J/mol K, respectively. The calculated results exhibit an asymptotic behavior toward the total magnetic entropy of spin-5/2 ($R \ln 6 \simeq 14.9$). Although the experimental temperature is not sufficient to observe the entire entropy shift, the temperature dependence of the experimental results is well reproduced by the entropy change from the higher temperature region.

Here, we considered the ground state of the present system. Our previous studies have demonstrated that MO calculations for verdazyl-based compounds reliably provide values of exchange interactions between radical spins, thus enabling the examination of their intrinsic behavior [15–18,20,21]. Accordingly, considering the MO evaluations, we assumed the exchange interactions as $J_2/J_1 = 0.63$ and $J_3/J_1 = 0.17$ K. Additionally, for the quantum Monte Carlo calculation [42], we fixed $J_4 = 0$ to avoid the negative sign problem, leading to a nonfrustrated case. Regarding $J_{\rm Mn}$, we assumed $J_{\rm Mn}/J_1 = 0.2$, as evaluated from the magnetization analysis above. We confirm that the 5/7 magnetization plateau appears up to approximately $H/J_1 = 1.15$, as shown in Fig. 4(a). Consequently, the observed plateau up to 60 T indicates that the actual value of J_1 is more than 70 K. Given that the magnetic

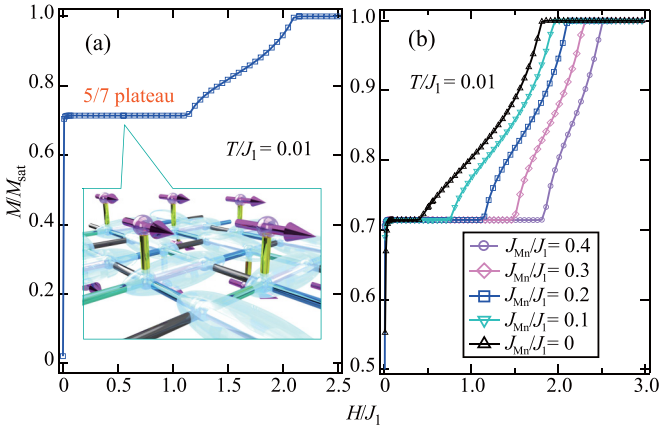

FIG. 4. (a) Calculated magnetization curve at $T/J_1 = 0.01$ for the expected spin model assuming the nonfrustrated case ($J_4 = 0$) with $J_2/J_1 = 0.63$, $J_3/J_1 = 0.17$ K, and $J_{Mn}/J_1 = 0.2$. The illustrations describe the singletlike quantum state protected by the fully polarized spin-5/2 in the plateau phase. (b) J_{Mn}/J_1 dependence of the normalized magnetization curve at $T/J_1 = 0.01$.

properties below the plateau phase can be described by the spin-5/2 monomer, the plateau is considered to form an AF quantum state with fully polarized spin-5/2 along the field direction. As the dominant AF interaction J_1 plays a crucial role and contributes more significantly than the other interactions, we anticipate the formation of a singletlike quantum state in the 2D plane, as schematically illustrated in Fig. 4(a).

Finally, we examine the stability of the quantum state in association with frustration and coupling with spin-5/2. Frustrated systems tend to lower their ground-state energies through lattice decouplings [46–50]. In the present lattice, the weakest ferromagnetic interaction J_4 is expected to be decoupled to minimize the energy loss due to frustration, thus stabilizing the singletlike quantum state. Moreover, ferromagnetic interactions are known to enhance the decoupling of the AF quantum state [23,51], which aligns well with the J_4 decoupling scenario. Accordingly, although it is difficult to quantitatively verify the precise effects of frustration, we can expect that the frustration acts to stabilize the quantum state in the present spin lattice. In terms of the effects of the coupling with spin-5/2, we calculated J_{Mn}/J_1 dependence of the magnetization curves with fixed $J_2/J_1 = 0.63$ and $J_3/J_1 = 0.17$ K, as shown in Fig. 4(b). We confirm that a case with no spin-5/2 coupling leads to a significant reduction in the plateau region. These findings indicate that the quantum state in the square lattice is highly stabilized by coupling with spin-5/2. This stabilization of the quantum state can be understood as a compensation effect, similar to the Jaccarino-Peterin mechanism for the magnetic field-induced superconductivity [29–31], where the external magnetic field compensates the internal magnetic field caused by the π-d interaction. In our case, the internal magnetic field induced by the fully polarized spin-5/2 through J_{Mn} compensates the external magnetic field in the plateau phase, resulting in the expansion of the plateau region with the singletlike quantum state as J_{Mn} increases.

In summary, we succeeded in synthesizing single crystals of the verdazyl-based salt (m-MePy-V)$_2$MnCl$_4$. MO calculations indicated the formation of a spin-1/2 spatially anisotropic frustrated square lattice partially coupled with spin-5/2. In the low-field region, the magnetizations and specific heats were well explained by a spin-5/2 monomer that becomes fully polarized at approximately 10 T. In the high-field measurement, we observed a large magnetization plateau exceeding 60 T, indicating a nonmagnetic quantum state formed by $S = 1/2$ spins in the square lattice. The numerical analysis demonstrated that the observed quantum state exhibits singletlike correlations due to the dominant AF interaction. Furthermore, we confirmed that the quantum state is strongly stabilized by coupling with spin-5/2, attributed to the compensation mechanism with the internal magnetic field induced by the fully polarized spin-5/2. Our study reveals a mechanism to stabilize quantum spin states in condensed materials and suggests a strategy to control the stability of quantum spin states in magnetic fields, which may inspire future technologies for quantum computation based on materials science.

We thank Y. Kono for valuable discussions. This research was partly supported by the Murata Science Foundation and KAKENHI (Grants No. 23K13065 and No. 23H01127). A part of this work was performed as the joint-research program of ISSP, the University of Tokyo and the Institute for Molecular Science.

[1] R. Raussendorf and H. J. Briegel, A one-way quantum computer, Phys. Rev. Lett. **86**, 5188 (2001).
[2] H. J. Briegel, D. E. Browne, W. Dur, R. Raussendorf, and M. Van den Nest, Measurement-based quantum computation, Nat. Phys. **5**, 19 (2009).
[3] P. W. Anderson, Resonating valence bonds: A new kind of insulator? Mater. Res. Bull. **8**, 153 (1973).
[4] A. Kitaev, Anyons in an exactly solved model and beyond, Ann. Phys. (NY) **321**, 2 (2006).
[5] N. Shannon, T. Momoi, and P. Sindzingre, Nematic order in square lattice frustrated ferromagnets, Phys. Rev. Lett. **96**, 027213 (2006).
[6] K. Takano, Spin-gap phase of a quantum spin system on a honeycomb lattice, Phys. Rev. B **74**, 140402(R) (2006).
[7] W. Li, S.-S. Gong, Y. Zhao, and G. Su, Quantum phase transition, $O(3)$ universality class, and phase diagram of the spin-1/2 Heisenberg antiferromagnet on a distorted honeycomb lattice: A tensor renormalization-group study, Phys. Rev. B **81**, 184427 (2010).
[8] Y.-Z. Huang, B. Xi, X. Chen, W. Li, Z.-C. Wang, and G. Su, Quantum phase transition, universality, and scaling behaviors in the spin-1/2 Heisenberg model with ferromagnetic and antiferromagnetic competing interactions on a honeycomb lattice, Phys. Rev. E **93**, 062110 (2016).

[9] K. Uematsu and H. Kawamura, Randomness-induced quantum spin liquid behavior in the $s = 1/2$ random J_1-J_2 Heisenberg antiferromagnet on the honeycomb lattice, J. Phys. Soc. Jpn. **86**, 044704 (2017).

[10] J. W. Bray, H. R. Hart, L. V. Interrante, I. S. Jacobs, J. S. Kasper, G. D. Watkins, S. H. Wee, and J. C. Bonner, Observation of a spin-Peierls transition in a Heisenberg antiferromagnetic linear-chain system, Phys. Rev. Lett. **35**, 744 (1975).

[11] S. I. Jacobs, J. W. Bray, H. R. Hart, L. V. Interrante, J. S. Kasper, G. D. Watkins, D. E. Prober, and J. C. Bonner, Spin-Peierls transitions in magnetic donor-acceptor compounds of tetrathiafulvalene (TTF) with bisdithiolene metal complexes, Phys. Rev. B **14**, 3036 (1976).

[12] M. Hase, I. Terasaki, and K. Uchinokura, Observation of the spin-Peierls transition in linear Cu^{2+} (spin-1/2) chains in an inorganic compound $CuGeO_3$, Phys. Rev. Lett. **70**, 3651 (1993).

[13] D. S. Chow, P. Wzietek, D. Fogliatti, B. Alavi, D. J. Tantillo, C. A. Merlic, and S. E. Brow, Singular behavior in the pressure-tuned competition between spin-Peierls and antiferromagnetic ground states of $(TMTTF)_2PF_6$, Phys. Rev. Lett. **81**, 3984 (1998).

[14] H. Yamaguchi, H. Takahashi, T. Kawakami, K. Okamoto, T. Sakai, T. Yajima, and Y. Iwasaki, Spin-Peierls transition to a Haldane phase, Phys. Rev. B **107**, L161111 (2023).

[15] H. Yamaguchi, K. Iwase, T. Ono, T. Shimokawa, H. Nakano, Y. Shimura, N. Kase, S. Kittaka, T. Sakakibara, T. Kawakami, and Y. Hosokoshi, Unconventional magnetic and thermodynamic properties of $S = 1/2$ spin ladder with ferromagnetic legs, Phys. Rev. Lett. **110**, 157205 (2013).

[16] H. Yamaguchi, M. Yoshida, M. Takigawa, K. Iwase, T. Ono, N. Kase, K. Araki, S. Kittaka, T. Sakakibara, T. Shimokawa, T. Okubo, K. Okunishi, A. Matsuo, and Y. Hosokoshi, Field-induced incommensurate phase in the strong-rung spin ladder with ferromagnetic legs, Phys. Rev. B **89**, 220402(R) (2014).

[17] H. Yamaguchi, H. Miyagai, Y. Kono, S. Kittaka, T. Sakakibara, K. Iwase, T. Ono, T. Shimokawa, and Y. Hosokoshi, Quantum phase near the saturation field in the $S = 1/2$ frustrated spin ladder, Phys. Rev. B **91**, 125104 (2015).

[18] H. Yamaguchi, T. Okubo, S. Kittaka, T. Sakakibara, K. Araki, K. Iwase, N. Amaya, T. Ono, and Y. Hosokoshi, Experimental realization of a quantum pentagonal lattice, Sci. Rep. **5**, 15327 (2015).

[19] H. Yamaguchi, M. Okada, Y. Kono, S. Kittaka, T. Sakakibara, T. Okabe, Y. Iwasaki, and Y. Hosokoshi, Randomness-induced quantum spin liquid on honeycomb lattice, Sci. Rep. **7**, 16144 (2017).

[20] H. Yamaguchi, Y. Tamekuni, Y. Iwasaki, and Y. Hosokoshi, Candidate for a fully frustrated square lattice in a verdazyl-based salt, Phys. Rev. B **97**, 201109(R) (2018).

[21] H. Yamaguchi, Y. Sasaki, T. Okubo, M. Yoshida, T. Kida, M. Hagiwara, Y. Kono, S. Kittaka, T. Sakakibara, M. Takigawa, Y. Iwasaki, and Y. Hosokoshi, Field-enhanced quantum fluctuation in an $S = 1/2$ frustrated square lattice, Phys. Rev. B **98**, 094402 (2018).

[22] H. Yamaguchi, Y. Iwasaki, Y. Kono, T. Okubo, S. Miyamoto, Y. Hosokoshi, A. Matsuo, T. Sakakibara, T. Kida, and M. Hagiwara, Quantum critical phenomena in a spin-1/2 frustrated square lattice with spatial anisotropy, Phys. Rev. B **103**, L220407 (2021).

[23] H. Yamaguchi, N. Uemoto, T. Okubo, Y. Kono, S. Kittaka, T. Sakakibara, T. Yajima, S. Shimono, Y. Iwasaki, and Y. Hosokoshi, Gapped ground state in a spin-1/2 frustrated square lattice, Phys. Rev. B **104**, L060411 (2021).

[24] Y. Iwasaki, T. Kida, M. Hagiwara, T. Kawakami, Y. Hosokoshi, Y. Tamekuni, and H. Yamaguchi, Effective $S = 2$ antiferromagnetic spin chain in the salt (o-MePy-V)$FeCl_4$, Phys. Rev. B **97**, 085113 (2018).

[25] Y. Iwasaki, T. Kida, M. Hagiwara, T. Kawakami, Y. Kono, S. Kittaka, T. Sakakibara, Y. Hosokoshi, and H. Yamaguchi, Field-induced quantum magnetism in the verdazyl-based charge-transfer salt [o-MePy-V-(p-Br)$_2$]$FeCl_4$, Phys. Rev. B **98**, 224411 (2018).

[26] H. Yamaguchi, T. Okita, Y. Iwasaki, Y. Kono, N. Uemoto, Y. Hosokoshi, T. Kida, T. Kawakami, A. Matsuo, and M. Hagiwara, Experimental realization of Lieb-Mattis plateau in a quantum spin chain, Sci. Rep. **10**, 9193 (2020).

[27] H. Yamaguchi, Y. Iwasaki, Y. Kono, T. Okita, A. Matsuo, M. Akaki, M. Hagiwara, and Y. Hosokoshi, Low-energy magnetic excitations in the mixed spin-(1/2, 5/2) chain, Phys. Rev. B **102**, 060408(R) (2020).

[28] H. Yamaguchi, T. Okita, Y. Iwasaki, Y. Kono, Y. Hosokoshi, T. Kida, A. Matsuo, T. Kawakami, and M. Hagiwara, Magnetic properties of a mixed spin-(1/2, 5/2) chain in (4-Cl-o-MePy-V)$FeCl_4$, J. Phys. Soc. Jpn. **90**, 064707 (2021).

[29] S. Uji, H. Shinagawa, T. Terashima, T. Yakabe, Y. Terai, M. Tokumoto, A. Kobayashi, H. Tanaka, and H. Kobayashi, Magnetic-field-induced superconductivity in a two-dimensional organic conductor, Nature (London) **410**, 908 (2001).

[30] T. Konoike, S. Uji, T. Terashima, M. Nishimura, S. Yasuzuka, K. Enomoto, H. Fujiwara, B. Zhang, and H. Kobayashi, Magnetic-field-induced superconductivity in the antiferromagnetic organic superconductor $\kappa-(BETS)_2FeBr_4$, Phys. Rev. B **70**, 094514 (2004).

[31] V. Jaccarino and M. Peter, Ultra-high-field superconductivity, Phys. Rev. Lett. **9**, 290 (1962).

[32] R. Kuhn, Über Verdazyle und verwandte Stickstoffradikale, Angew Chem. **76**, 691 (1964).

[33] S. Miyamoto, Y. Iwasaki, N. Uemoto, Y. Hosokoshi, H. Fujiwara, S. Shimono, and H. Yamaguchi, Magnetic properties of honeycomb-based spin models in verdazyl-based salts, Phys. Rev. Mater. **3**, 064410 (2019).

[34] See Supplemental Material at http://link.aps.org/supplemental/10.1103/PhysRevB.109.L100404 for detailed crystallographic parameters and molecular pairs associated with the intermolecular exchange interactions.

[35] The MO calculations were performed using the UB3LYP method in the Gaussian 09 program package. The basis sets are 6-31G between radicals and 6-31G(d, p) for π-d couplings. For the estimation of intermolecular magnetic interaction, we applied the previously reported evaluation scheme [36].

[36] M. Shoji, K. Koizumi, Y. Kitagawa, T. Kawakami, S. Yamanaka, M. Okumura, and K. Yamaguchi, A general algorithm for calculation of Heisenberg exchange integrals J in multispin systems, Chem. Phys. Lett. **432**, 343 (2006).

[37] A. Gleizes and M. Verdaguer, Ordered magnetic bimetallic chains: a novel class of one-dimensional compounds, J. Am. Chem. Soc. **103**, 7373 (1981).

[38] O. Kahn, Y. Pei, M. Verdaguer, J. P. Renard, and J. Sletten, Magnetic ordering of manganese(II) copper(II) bimetallic

chains; design of a molecular based ferromagnet, J. Am. Chem. Soc. **110**, 782 (1988).

[39] M. Hagiwara, K. Minami, Y. Narumi, K. Tatani, and K. Kindo, Magnetic properties of a quantum ferrimagnet: $NiCu(pba)(D_2O)_3{\cdot}2D_2O$, J. Phys. Soc. Jpn. **67**, 2209 (1998).

[40] H. Yamaguchi, Y. Tamekuni, Y. Iwasaki, R. Otsuka, Y. Hosokoshi, T. Kida, and M. Hagiwara, Magnetic properties of a quasi-two-dimensional $S = 1/2$ Heisenberg antiferromagnet with distorted square lattice, Phys. Rev. B **95**, 235135 (2017).

[41] N. Uemoto, Y. Kono, S. Kittaka, T. Sakakibara, T. Yajima, Y. Iwasaki, S. Miyamoto, Y. Hosokoshi, and H. Yamaguchi, $S = 1/2$ ferromagnetic Heisenberg chain in a verdazyl-based complex, Phys. Rev. B **99**, 094418 (2019).

[42] The QMC code is based on the directed loop algorithm in the stochastic series expansion representation [43]. The spin model unit contains eight radical sites with spin-1/2 and four Mn sites with spin-5/2. The calculations was performed for $N = 768$ under the periodic boundary condition, where N denotes the system size. It was confirmed that there is no significant size-dependent effect. The number of sweeps is 50000 beginning after 10000 sweep thermalization. All calculations were carried out using the ALPS application [44,45].

[43] A. W. Sandvik, Stochastic series expansion method with operator-loop update, Phys. Rev. B **59**, R14157 (1999).

[44] A. F. Albuquerque, F. Alet, P. Corboz, P. Dayal, A. Feiguin, L. Gamper, E. Gull, S. Gurtler, A. Honecker, R. Igarashi, M. Korner, A. Kozhevnikov, A. Lauchli, S. R. Manmana, M. Matsumoto, I. P. McCulloch, F. Michel, R. M. Noack, G. Pawlowski, L. Pollet *et al.*, The ALPS project release 1.3: Open-source software for strongly correlated systems, J. Magn. Magn. Mater. **310**, 1187 (2007).

[45] B. Bauer, L. D. Carr, A. Feiguin, J. Freire, S. Fuchs, L. Gamper, J. Gukelberger, E. Gull, S. Guertler, A. Hehn, R. Igarashi, S. V. Isakov, D. Koop, P. N. Ma, P. Mates, H. Matsuo, O. Parcollet, G. Pawlowski, J. D. Picon, L. Pollet *et al.*, The ALPS project release 2.0: open source software for strongly correlated systems, J. Stat. Mech.: Theory Exp. (2011) P05001.

[46] R. Coldea, D. A. Tennant, A. M. Tsvelik, and Z. Tylczynski, Experimental realization of a 2D fractional quantum spin liquid, Phys. Rev. Lett. **86**, 1335 (2001).

[47] R. Coldea, D. A. Tennant, and Z. Tylczynski, Extended scattering continua characteristic of spin fractionalization in the two-dimensional frustrated quantum magnet Cs_2CuCl_4 observed by neutron scattering, Phys. Rev. B **68**, 134424 (2003).

[48] S. Yunoki and S. Sorella, Two spin liquid phases in the spatially anisotropic triangular Heisenberg model, Phys. Rev. B **74**, 014408 (2006).

[49] W. Zheng, J. O. Fjærestad, R. R. P. Singh, R. H. McKenzie, and R. Coldea, Anomalous excitation spectra of frustrated quantum antiferromagnets, Phys. Rev. Lett. **96**, 057201 (2006).

[50] M. Kohno, O. A. Starykh, and L. Balents, Spinons and triplons in spatially anisotropic frustrated antiferromagnets, Nat. Phys. **3**, 790 (2007).

[51] M. Hagiwara, Y. Narumi, K. Minami, K. Kindo, H. Kitazawa, H. Suzuki, N. Tsujii, and H. Abe, Magnetization process of an $S = 1/2$ tetramer chain with ferromagnetic-ferromagnetic-antiferromagnetic-antiferromagnetic bond alternating interactions, J. Phys. Soc. Jpn. **72**, 943 (2003).